

# Short-term Transmission Maintenance Scheduling Considering Network Topology Optimization

Weixin Zhang, Bo Hu, Kaigui Xie, Changzheng Shao, Tao Niu, Jiahao Yan, Lvbin Peng, Maosen Cao, and Yue Sun

**Abstract**—With the increasing penetration of renewable energy sources, transmission maintenance scheduling (TMS) will have a larger impact on the accommodation of wind power. Meanwhile, the more flexible transmission network topology owing to the network topology optimization (NTO) technique can ensure the secure and economic operation of power systems. This paper proposes a TMS model considering NTO to decrease the wind curtailment without adding control devices. The problem is formulated as a two-stage stochastic mixed-integer programming model. The first stage arranges the maintenance periods of transmission lines. The second stage optimizes the transmission network topology to minimize the maintenance cost and system operation in different wind speed scenarios. The proposed model cannot be solved efficiently with off-the-shelf solvers due to the binary variables in both stages. Therefore, the progressive hedging algorithm is applied. The results on the modified IEEE RTS-79 system show that the proposed method can reduce the negative impact of transmission maintenance on wind accommodation by 65.49%, which proves its effectiveness.

**Index Terms**—Mixed-integer linear programming, network topology optimization, progressive hedging algorithm, stochastic optimization, transmission maintenance scheduling, wind curtailment.

## NOMENCLATURE

### A. Indices

$d$	Index of load buses from 1 to $D$
$g$	Index of units from 1 to $G$
$l$	Index of lines that need maintenance from 1 to $L$
$s$	Index of typical scenarios from 1 to $S$
$t$	Index of research periods from 1 to $T$

Manuscript received: October 28, 2020; revised: March 14, 2021; accepted: May 17, 2021. Date of CrossCheck: May 17, 2021. Date of online publication: July 14, 2021.

This work was supported by the National Key R&D Program of China “Technology and application of wind power/photovoltaic power prediction for promoting renewable energy consumption” (No. 2018YFB0904200) and eponymous Complement S&T Program of State Grid Corporation of China (No. SGLND-KOOKJJS1800266).

This article is distributed under the terms of the Creative Commons Attribution 4.0 International License (<http://creativecommons.org/licenses/by/4.0/>).

W. Zhang, B. Hu (corresponding author), K. Xie, C. Shao, T. Niu, J. Yan, L. Peng, M. Cao, and Y. Sun are with the State Key Laboratory of Power Transmission Equipment & System Security and New Technology at Chongqing University, Chongqing 400044, China (e-mail: weixinzhang@cqu.edu.cn; hboy8361@163.com; kaiguixie@vip.163.com; cshao@cqu.edu.cn; niutthu@qq.com; yanjiahaojia@163.com; lvpeng1210@outlook.com; cms517499119@outlook.com; 281232348@qq.com).

DOI: 10.35833/MPCE.2020.000937

$w$  Index of wind farms from 1 to  $W$

### B. Constants

$\pi^s$	Probability of typical scenario $s$
$\theta^{\max}$	The maximum phase angle difference
$B$	Number of buses
$b_l$	Susceptance of line $l$
$c_{l,t}$	Maintenance cost of line $l$ during period $t$
$c_g$	Marginal cost of conventional unit $g$
$c_w$	Unit cost of wind curtailment of wind farm $w$
$c_d$	Unit cost of load shedding of load bus $d$
$D$	Number of load buses
$e_l$	The earliest period to begin maintenance of line $l$
$G$	Number of conventional units
$L$	Number of lines that need maintenance
$l_l$	The latest period to finish maintenance of line $l$
$M_l$	A large enough constant
$n$	The maximum number of concurrent bus-bar splitting during period $t$
$P_g^{\min}$	Lower limit of real power generation of unit $g$
$P_g^{\max}$	Upper limit of real power generation of unit $g$
$P_{d,t}$	Load demand of load bus $d$ during period $t$
$P_{w,t}$	Real power generation of wind farm $w$ during period $t$
$P_l^{\max}$	The maximum capacity of line $l$
$S$	Number of typical scenarios
$T$	Number of time periods
$W$	Number of wind farms
$X_l$	Number of time periods required for maintenance of line $l$
$X_t^{\max}$	The maximum number of concurrent transmission maintenances during period $t$
<b>C. Sets</b>	
$D_b$	Set of load buses connected to substation $b$
$G_b$	Set of units connected to substation $b$
$L_b$	Set of lines connected to substation $b$
$LF_b$	Set of lines flow from substation $b$
$LT_b$	Set of lines flow to substation $b$



$W_b$	Set of wind farms connected to substation $b$
<i>D. Variables</i>	
$\theta_{b,i}^s$	Phase angle of bus-bar $i$ ( $i = 1, 2$ ) of substation $b$ during period $t$ in typical scenario $s$
$\theta_{l,e,t}^s$	Phase angle of line $l$ at the side of $e$ ( $e = fr, to$ , where $fr$ means starting bus, $to$ means end bus) during period $t$ in typical scenario $s$
$\theta_{l,e,t,i}^s$	Phase angle of line $l$ at the side of $e$ ( $e = fr, to$ ) connected to bus-bar $i$ ( $i = 1, 2$ ) during period $t$ in typical scenario $s$
$P_{g,t}^s$	Real power generation of unit $g$ during period $t$ in typical scenario $s$
$P_{g,t,i}^s$	Real power generation of unit $g$ connected to bus-bar $i$ ( $i = 1, 2$ ) during period $t$ in typical scenario $s$
$P_{d,t,i}^s$	Load demand of load bus $d$ connected to bus-bar $i$ ( $i = 1, 2$ ) during period $t$ in typical scenario $s$
$P_{w,t,i}^s$	Real power generation of wind farm $w$ connected to bus-bar $i$ ( $i = 1, 2$ ) during period $t$ in typical scenario $s$
$\tilde{P}_{d,t}^s$	Load shedding of load bus $d$ during period $t$ in typical scenario $s$
$\tilde{P}_{d,t,i}^s$	Load shedding of load bus $d$ connected to bus-bar $i$ ( $i = 1, 2$ ) during period $t$ in typical scenario $s$
$\tilde{P}_{w,t}^s$	Wind curtailment of wind farm $w$ during period $t$ in typical scenario $s$
$\tilde{P}_{w,t,i}^s$	Wind curtailment of wind farm $w$ connected to bus-bar $i$ ( $i = 1, 2$ ) during period $t$ in typical scenario $s$
$P_{l,t}^s$	Power flow of line $l$ during period $t$ in typical scenario $s$
$P_{l,e,t,i}^s$	Power flow of line $l$ at the side of $e$ ( $e = fr, to$ ) during period $t$ through bus-bar $i$ ( $i = 1, 2$ ) in typical scenario $s$
$x_{l,t}$	Binary variables representing state of line $l$ during period $t$ (0 if line is open, otherwise 1)
$x_{l,e,t}^s$	Binary variables representing connection status of line $l$ at the side of $e$ ( $e = fr, to$ ) during period $t$ (0 if it is connected to bus-bar 1, otherwise bus-bar 2) in typical scenario $s$
$y_{b,t}^s$	Binary variables representing state of bus-bar in substation $b$ (0 if bus-bar is splitting, otherwise 1) in typical scenario $s$
$y_{g,t}^s$	Binary variables representing connection status of unit $g$ during period $t$ (0 if it is connected to bus-bar 1, otherwise bus-bar 2) in typical scenario $s$
$y_{w,t}^s$	Binary variables representing connection status of wind farm $w$ during period $t$ (0 if it is connected to bus-bar 1, otherwise bus-bar 2) in typical scenario $s$
$y_{d,t}^s$	Binary variables representing connection status of load bus $d$ during period $t$ (0 if it is connected to bus-bar 1, otherwise bus-bar 2) in typical scenario $s$

## I. INTRODUCTION

WITH the growth of renewable energy capacity around the world, the past decade has witnessed great change in the energy supply mix. However, large portions of wind power are curtailed due to the technical limitations of power system operations. Among these limitations, transmission congestion accounts for a significant portion of wind curtailment [1], [2].

From the perspective of power transmission systems, both the insufficient capacity of transmission lines and underutilization of transmission lines due to systemwide transmission congestion are the causes of wind curtailment [2]. Mostly, the transmission congestion has been triggered by line outages, including forced outages due to contingencies or scheduled outages due to transmission maintenance scheduling (TMS) [3]. Therefore, if TMS is not designed properly, it is likely to cause transmission congestion and further lead to a large amount of wind curtailment.

Many research works have focused on the field of TMS. Generally, TMS is addressed jointly with generation maintenance scheduling (GMS) [4]. In [5], a generation and transmission maintenance scheduling (G&TMS) model considering network security constraints is established. The Benders decomposition technique is used to solve the problem due to its complexity. Emission limitations and fuel supply constraints are further considered in [6] based on the model in [5]. Transmission constraints and forced outage rates are considered in [7]. The Lagrange relaxation method and Benders decomposition technique are used for transmission constrained price and line maintenance. In [8], a G&TMS model considering  $N-1$  contingencies is proposed. The Benders decomposition technique is also employed to decompose the problem into a master problem and several subproblems. Furthermore, the relaxation induced algorithm is used to efficiently solve the computationally burdensome master problem. In [9] and [10], a G&TMS model based on security-constrained unit commitment is proposed. It can be decomposed into mid-term GMS, TMS, and short-term security-constrained unit commitment problems. These problems are co-optimized to effectively improve the system security during the maintenance period. In [11], a G&TMS model based on an hourly basis is proposed. The algorithm called teaching learning based optimization is proposed for solving the integrated maintenance scheduling problem. In [12], covariates such as equipment aging, critical equipment outage, and extreme weather are further considered during the maintenance. Their influences on maintenance are quantified through a Monte Carlo based framework.

TMS can also be addressed independently from GMS. In [13], TMS is solved by the genetic algorithm. A short-term TMS model is proposed in [14]. It is decomposed into a master problem and two subproblems. The maintenance scheduling is solved in the master problem, while the transmission/voltage constraints are considered in the subproblems separately. In [15], a bilevel model of TMS on a yearly basis is proposed. The upper layer aims to maximize the transmission capacity, while the lower layer aims to maxi-

imize the social welfare. Finally, the bilevel model is solved after it is transferred into a mixed-integer linear programming (MILP) problem. The load shedding and  $N-1$  contingency analysis are considered in the TMS model in [16]. At present, the wind power accommodation is rarely considered in the TMS model. In [17], the robust optimization is used to cope with the uncertainty of wind power. However, it is mainly focused on the solution efficiency rather than the reduction of wind curtailment.

The purpose of this paper is to alleviate the negative impact of TMS on wind power accommodation. The transmission network is conventionally regarded as a static structure. In other words, its topology does not change with operation conditions unless the equipment is damaged or out of service for maintenance. However, it has been reported that network topology optimization (NTO) can ensure the secure and economical operation of the power system [18]. Thus, NTO is introduced to relieve the issue of transmission congestion in TMS.

NTO includes the optimal transmission switching (OTS) [19] and bus-bar splitting (BBS) [20]. In [21], OTS and BBS are used as correction mechanisms to alleviate the occasional overload of transmission lines, and a heuristic algorithm is used to solve the problem. OTS is used as a tool for the congestion management in [22]. The goal of the model is to minimize the overload of transmission lines. Both genetic algorithms and deterministic methods are used to solve this problem. In [20], OTS and BBS are adopted as corrective measures to alleviate the overload and overvoltage of transmission lines. Sparse techniques and fast decoupling power flow are used to reduce the number of iterations required, which results in faster identification of the best switching operations. In [23], OTS and the day-ahead unit commitment are co-optimized to relieve the transmission congestion and reduce the generation cost using switching operations. BBS and OTS are combined to establish a unified NTO model in [24]. The coordination between BBS and OTS can be realized by modifying the parameters of the mathematical model. The results show that the NTO model can effectively relieve transmission congestion and reduce the operation cost. However, NTO has not been considered to reduce wind curtailment in previous research works on TMS.

In this paper, a TMS approach considering NTO is proposed and formulated as a two-stage stochastic mixed-integer programming (SMIP) model. In the first stage, the system planner makes maintenance arrangements for transmission lines. The second stage optimizes the transmission network topology and evaluates the maintenance cost and system operation cost considering various wind speed scenarios. The wind power accommodation in different wind speed scenarios is measured by wind curtailment penalty cost.

The operation statuses of transmission lines and NTO decisions are represented as integer variables in the first and second stages of the proposed model, respectively, which result in computational complexity. The ad-hoc MILP solvers cannot be directly used to solve the proposed model. To solve

the problem, the progressive hedging (PH) algorithm [25], [26] is adopted to effectively solve the two-stage SMIP model. The PH algorithm has been widely implemented in kinds of problems in power systems [27], [28]. Unlike the commonly used Benders decomposition, the PH algorithm does not need any special form of the second stage. The first- and second-stage decisions are not made separately. Instead, the original problem is detached into scenario-based subproblems, and the first- and second-stage decisions are co-optimized for each scenario independently. Moreover, the parallel solution of subproblems enables higher computational efficiency.

The main contributions of this paper are listed as follows.

1) A two-stage SMIP model is proposed to cope with wind curtailment in TMS. The proposed model obtains the sequence of maintenance for different transmission lines and determines the optimal topology of the transmission network during maintenance, which can efficiently relieve the transmission congestion and reduce the wind curtailment.

2) The PH algorithm is introduced to deal with the large-scale two-stage SMIP model. The PH algorithm can decompose the original problem into small-scale scenario-based subproblems and solve them in parallel, thereby reducing the computational complexity.

The remainder of this paper is organized as follows. Section II shows the mathematical formulation of the proposed model. Section III introduces the solution algorithm. The results and analysis for the modified IEEE RTS-79 system are discussed in Section IV. Section V concludes this paper.

## II. MATHEMATICAL FORMULATION

A two-stage SMIP model is proposed for the short-term TMS approach considering NTO under uncertainty. The first stage is to make TMS decisions (operation status of transmission lines in each period), and the second stage is to make NTO decisions and evaluate operation costs in terms of conventional generation output, wind curtailment, and load shedding in realized wind speed scenarios. Some reasonable assumptions are first made about the proposed model. The mechanism of NTO is then discussed, followed by the overall mathematical formulation of the model together with the construction method of wind speed scenarios.

### A. Model Assumption

The following assumptions are made in the proposed model.

1) The system components are reliable during maintenance, i.e., random failures of components are not considered.

2) The total length of the planning period is a week, which is divided into  $7 \times 24$  time periods. The average wind speed and the average load in each hour are regarded as the wind speed and load for the corresponding period.

3) For simplicity, the load demand profile is the same as historical data. In other words, the load uncertainty is not considered.

4) All conventional generation units are turned on during

the planning horizon. Therefore, the minimum on/off time constraints can be ignored.

### B. Mechanism of NTO

High-voltage substations are critical infrastructures that transfer electric energy from the power source side to the users' side at various voltage levels. NTO is used to change the connections between different components through the operations of circuit breakers (CBs) inside the substations. This mechanism of NTO can be illustrated with the breaker-and-a-half substation arrangement in Fig. 1.

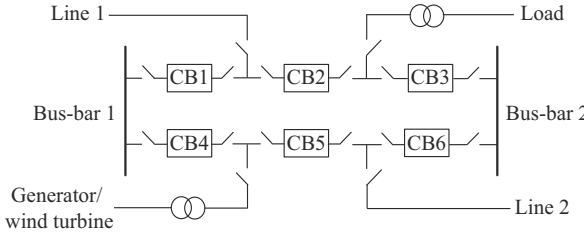


Fig. 1. Breaker-and-a-half substation arrangement.

The breaker-and-a-half substation arrangement consists of two bus-bars, both of which are normally energized. In a string, three CBs connect the two bus-bars, and between each two CBs, there is a circuit. In this arrangement, three CBs are used in two independent circuits. Hence, the two circuits share a CB as the common center, so each circuit has 1.5 CBs [29].

All CBs are put into operation under normal conditions. When switching a line, two CBs must be open. For example, switching line 1 requires opening CB1 and CB2. When splitting a bus-bar, it is necessary to open at least one CB in each set of CBs. For example, the splitting of bus-bar 1 and bus-bar 2 requires the opening of CB2 and CB5. In this way, line 1 and the generator/wind turbine can be connected to bus-bar 1, while line 2 and the load can be connected to bus-bar 2. Based on the above analysis, a generalized substation model can be established, as shown in Fig. 2.

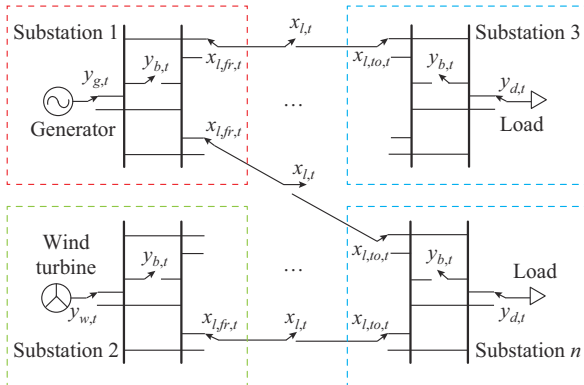


Fig. 2. Generalized substation model.

Then, the NTO mathematical model is formulated based on the generalized substation model. In Fig. 2, each substation is composed of two bus-bars, and the power sources

(conventional units/wind farms), transmission lines, and loads can be connected to either bus-bar 1 or bus-bar 2. NTO allows line switching and bus-bar splitting. In the mathematical formulation, the connection statuses of these components are represented as the values of binary variables.

### C. Optimization Model

In this two-stage SMIP model, the objective is to minimize the expected costs over all time periods, including the maintenance cost and operation cost (conventional generation cost, wind curtailment cost, and load shedding cost) weighted by the probability of each scenario, as shown in (1). There are totally five maintenance scheduling constraints that should be considered in the first stage. Constraint (2) specifies the total time required for the maintenance of each line. Constraint (3) states the earliest start time and the latest end time for the maintenance of each line. Constraint (4) ensures the continuity of the maintenance. Once a maintenance activity begins, it will not stop until completed. Constraint (5) limits the number of lines that can be switched for maintenance, which depends on the maintenance resources. Constraint (6) ensures the priority of the lines for maintenance.

$$\min \sum_{l=1}^L \sum_{t=1}^T c_{l,t} (1 - x_{l,t}) + \mathbb{E}_s (\phi(s)) \quad (1)$$

s.t.

$$\sum_{t=1}^T (1 - x_{l,t}) = X_l \quad (2)$$

$$\begin{cases} x_{l,t} \in \{0, 1\} & e_l \leq t \leq l_l \\ x_{l,t} = 1 & \text{else} \end{cases} \quad (3)$$

$$x_{l,t} - x_{l,t+1} \leq 1 - x_{l,t+\tau} \quad \tau = 2, 3, \dots, X_l \quad (4)$$

$$\sum_{l=1}^L (1 - x_{l,t}) \leq X_t^{\max} \quad (5)$$

$$\sum_{t=1}^T (1 - x_{l,t}) \geq 1 - x_{j,t} \quad (6)$$

The expected operation cost is obtained by solving the second-stage problem in (7). For a fixed value of first-stage decision variables  $\mathbf{x}$  and a realized typical scenario  $s$ , the second-stage problem can be formulated as (8)-(36).

$$\mathbb{E}_s (\phi(s)) = \sum_s \pi^s \phi(s) \quad (7)$$

$$\phi(s) = \min \left\{ \sum_{t=1}^T \sum_{g=1}^G c_g P_{g,t}^s + \sum_{t=1}^T \sum_{w=1}^W c_w \tilde{P}_{w,t}^s + \sum_{t=1}^T \sum_{d=1}^D c_d \tilde{P}_{d,t}^s \right\} \quad (8)$$

s.t.

$$(1 - y_{g,t}^s) P_{g,t}^{\min} \leq P_{g,t,1}^s \leq (1 - y_{g,t}^s) P_{g,t}^{\max} \quad (9)$$

$$y_{g,t}^s P_{g,t}^{\min} \leq P_{g,t,2}^s \leq y_{g,t}^s P_{g,t}^{\max} \quad (10)$$

$$P_{g,t}^s = P_{g,t,1}^s + P_{g,t,2}^s \quad (11)$$

$$P_{d,t,1}^s = (1 - y_{d,t}^s) P_{d,t}^s \quad (12)$$

$$P_{d,t,2}^s = y_{d,t}^s P_{d,t}^s \quad (13)$$

$$0 \leq \tilde{P}_{d,t,i}^s \leq P_{d,t,i}^s \quad i = 1, 2 \quad (14)$$

$$\begin{aligned}
& \tilde{P}_{d,t}^s = \tilde{P}_{d,t,1}^s + \tilde{P}_{d,t,2}^s & (15) \\
& P_{w,t,1}^s = (1 - y_{w,t}^s) P_{w,t} & (16) \\
& P_{w,t,2}^s = y_{w,t}^s P_{w,t} & (17) \\
& 0 \leq \tilde{P}_{w,t,i}^s \leq P_{w,t,i}^s \quad i = 1, 2 & (18) \\
& \tilde{P}_{w,t}^s = \tilde{P}_{w,t,1}^s + \tilde{P}_{w,t,2}^s & (19) \\
& -x_{l,t} (1 - x_{l,e,t}^s) P_l^{\max} \leq P_{l,e,t,1}^s \leq x_{l,t} (1 - x_{l,e,t}^s) P_l^{\max} \quad \forall e & (20) \\
& -x_{l,t} x_{l,e,t}^s P_l^{\max} \leq P_{l,e,t,2}^s \leq x_{l,t} x_{l,e,t}^s P_l^{\max} \quad \forall e & (21) \\
& P_{l,t}^s = P_{l,e,t,1}^s + P_{l,e,t,2}^s \quad \forall e & (22) \\
& -\theta^{\max} (1 - y_{b,t}^s) \leq \theta_{b,t,1}^s - \theta_{b,t,2}^s \leq \theta^{\max} (1 - y_{b,t}^s) & (23) \\
& -x_{l,e,t}^s \theta^{\max} \leq \theta_{l,e,t}^s - \theta_{l,e,t,1}^s \leq x_{l,e,t}^s \theta^{\max} \quad \forall e & (24) \\
& -(1 - x_{l,e,t}^s) \theta^{\max} \leq \theta_{l,e,t}^s - \theta_{l,e,t,2}^s \leq (1 - x_{l,e,t}^s) \theta^{\max} \quad \forall e & (25) \\
& -x_{l,e,t}^s \theta^{\max} \leq \theta_{l,e,t,1}^s - \theta_{l,t,1}^s \leq x_{l,e,t}^s \theta^{\max} \quad k = (l, e) & (26) \\
& -(1 - x_{l,e,t}^s) \theta^{\max} \leq \theta_{l,e,t,2}^s - \theta_{l,t,2}^s \leq (1 - x_{l,e,t}^s) \theta^{\max} \quad k = (l, e) & (27) \\
& y_{b,t}^s - 1 + y_{g,t}^s \leq 0 & (28) \\
& y_{b,t}^s - 1 + y_{d,t}^s \leq 0 & (29) \\
& y_{b,t}^s - 1 + y_{w,t}^s \leq 0 & (30) \\
& y_{b,t}^s - 1 + x_{l,e,t}^s \leq 0 \quad \forall e & (31) \\
& \sum_{l \in L_b} x_{l,e,t}^s \geq 2(1 - y_{b,t}^s) \quad \forall e & (32) \\
& \sum_{l \in L_b} (1 - x_{l,e,t}^s) - \sum_{l \in L_b} (1 - x_{l,t}^s) \geq 2(1 - y_{b,t}^s) \quad \forall e & (33) \\
& \sum_b (1 - y_{b,t}^s) \leq n & (34) \\
& \sum_{g \in G_b} P_{g,t,i}^s + \sum_{w \in W_b} (P_{w,t,i}^s - \tilde{P}_{w,t,i}^s) - \sum_{l \in LF_b} P_{l,fr,t,i}^s + \sum_{l \in LT_b} P_{l,to,t,i}^s = \\
& \sum_{d \in D_b} (P_{d,t,i}^s - \tilde{P}_{d,t,i}^s) \quad i = 1, 2 & (35) \\
& -M_l (1 - x_{l,t}^s) \leq (\theta_{l,fr,t}^s - \theta_{l,to,t}^s) b_l - P_{l,t}^s \leq M_l (1 - x_{l,t}^s) & (36)
\end{aligned}$$

Equation (8) represents the objective function of the second-stage problem, i.e., minimizing the operation cost in a realized wind speed scenario. The mathematical model of NTO mainly includes constraints (9)-(34).

Constraints (9) and (10) determine the connecting status of unit  $g$ . When a unit is connected to one bus-bar, the power generation on the other bus-bar must be forced to be 0. Similarly, constraints (12), (13) and constraints (16), (17) determine the connecting statuses of loads and wind farms, respectively. Constraint (11) represents the output of conventional units. Constraints (14) and (15) limit the amount of load shedding. Constraints (18) and (19) limit the amount of wind curtailment.

Constraints (20) and (21) determine the power flow through each end side of line  $l$ . When line  $l$  is open, i.e.,  $x_{l,t} = 0$ , there is no power flow at both sides of line  $l$ , which is independent of the connection position. When line  $l$  is closed, the connecting status of line  $l$  is defined similarly to con-

straints (9) and (10). Constraint (22) states that the power flow through line  $l$  is equal to that at each side of line  $l$ .

Constraint (23) means that the phase angle of each bus-bar must be equal when the bus-bars are not split. Otherwise, (23) is not a binding constraint. Constraints (24)-(27) indicate that the phase angle at each side of the line is equal to the phase angle of the bus-bar to which it is connected.  $k = (l, e)$  means the substation  $k$  is at the side of  $e$  of line  $l$ .

Constraints (28) - (31) indicate that conventional units, wind farms, loads, and lines can be connected to any bus-bar. However, when the bus-bars are not split, they are connected to both bus-bars at the same time. In this situation, the components are connected to bus-bar 1 by default. Constraints (32) and (33) indicate that only substations with more than two lines or branches connected to each bus-bar after BBS are allowed to be split. These constraints ensure the connectivity of the network when a contingency occurs. Meanwhile, if a transmission line is switched for maintenance, some bus-bars may not be allowed to be split in a certain scenario because of the requirement of the number of lines, i.e., more than two lines, connected to each bus-bar after BBS. For example, if a bus-bar has only four lines connected to it, it cannot be split when one of these four lines is under maintenance. These two constraints link the first-stage decisions with the second-stage variables. Moreover, the choice of the substation to be split is limited, which reduces the solution space and computational complexity. Constraint (34) limits the maximum number of substations that can be split at the same time.

In addition, power flow should be satisfied during maintenance. Constraint (35) ensures the power balance on each bus node. Constraint (36) determines the power flow on each line. When a line is switched for maintenance, its power flow will be forced to be 0. Otherwise,  $P_{l,t} = (\theta_{l,fr,t} - \theta_{l,to,t}) b_l$  will be satisfied.

The multiplications of two binary variables in constraints (20) and (21) result in nonlinear constraints and need to be linearized. Since these constraints have the same structure, they can be linearized by the same approach. Some auxiliary variables are introduced to linearize the original nonlinear constraints. Taking constraint (20) as an example, the linearization process is as follows:

$$\alpha_{l,e,t} \leq x_{l,t} \quad (37)$$

$$\alpha_{l,e,t} \leq 1 - x_{l,e,t} \quad (38)$$

$$\alpha_{l,e,t} \geq x_{l,t} - x_{l,e,t} \quad (39)$$

$$-\alpha_{l,e,t} P_l^{\max} \leq P_{l,e,t,1}^s \leq \alpha_{l,e,t} P_l^{\max} \quad (40)$$

#### D. Scenario Generation

The prediction of wind speed is not the focus of this paper. Therefore, typical scenarios are generated based on the historical wind speed data using the simultaneous backward reduction [30], which should be run before solving the two-stage SMIP model.

### III. SOLUTION ALGORITHM

The proposed two-stage SMIP model is computationally intractable due to the co-optimization of multi-period TMS decisions and the NTO decisions considering various scenarios. Off-the-shelf solvers can be used to solve the model, but will lead to the excessive computation time when a large number of scenarios are included. Therefore, the PH algorithm is applied to solve the proposed problem efficiently.

#### A. Compact Notation of Original Problem

To illustrate how the PH algorithm works, a compact notation is used to express the TMS model:

$$\min_{\mathbf{x}} \left( \mathbf{c}^T \mathbf{x} + \sum_s \pi^s \phi(\mathbf{x}, s) \right) \quad (41)$$

s.t.

$$\mathbf{A}\mathbf{x} \leq \mathbf{b} \quad (42)$$

$$\mathbf{x} \in \mathbb{Z}_+^{L \times T} \quad (43)$$

The vector  $\mathbf{c}$  represents the cost coefficient. The vectors  $\mathbf{A}$  and  $\mathbf{b}$  represent the associated parameters. Constraint (42) is a vector-form representation of the maintenance scheduling constraints (2)-(6).  $\phi(\mathbf{x}, s)$  represents the system operation problem in a given wind speed scenario, which can be rewritten as:

$$\phi(\mathbf{x}, s) = \min(\mathbf{p}^T \mathbf{y}) \quad (44)$$

s.t.

$$\mathbf{F}\mathbf{y} + \mathbf{G}(s)\mathbf{x} \leq \mathbf{H}(s) \quad (45)$$

$$\mathbf{y} \in \mathbb{Z}_+^{(B+G+W+D) \times T} \quad (46)$$

The vector  $\mathbf{y}$  represents the binary decision variables in the second stage. The vector  $\mathbf{p}$  represents the cost coefficient. The vectors  $\mathbf{F}$ ,  $\mathbf{G}(s)$ , and  $\mathbf{H}(s)$  represent the associated parameters, where  $\mathbf{G}(s)$  and  $\mathbf{H}(s)$  are related to scenario  $s$ . Constraint (45) is a vector-form representation of constraints (9)-(36).

The model defined by (41)-(46) can be written as a large-scale deterministic MILP model when there is a finite number of scenarios. The so-called extensive form (EF) of a two-stage SMIP model is given as:

$$z = \min \left\{ \mathbf{c}^T \mathbf{x} + \sum_s \pi^s (\mathbf{p}(s))^T \mathbf{y}(s) : (\mathbf{x}, \mathbf{y}(s)) \in \mathcal{Q}(s), s = 1, 2, \dots, S \right\} \quad (47)$$

where  $\mathcal{Q}(s) = \{(\mathbf{x}, \mathbf{y}(s)) : \mathbf{A}\mathbf{x} \leq \mathbf{b}, \mathbf{x} \in \mathbb{Z}_+^{L \times T}, \mathbf{F}\mathbf{y} + \mathbf{G}(s)\mathbf{x} \leq \mathbf{H}(s), \mathbf{y} \in \mathbb{Z}_+^{(B+G+W+D) \times T}\}$ . Here,  $\mathbf{x}$  is scenario independent, i.e., the non-anticipativity constraint  $\mathbf{x}(1) = \mathbf{x}(2) = \dots = \mathbf{x}(S)$  is enforced.  $\mathbf{p}(s)$  represents the  $s^{\text{th}}$  component of vector  $\mathbf{p}$ .  $\mathbf{y}(s)$  represents the scenario-specific decision vector of the second stage given  $\mathbf{x}$  and a particular scenario  $s$ .

#### B. PH Algorithm

It is time-consuming to directly solve the EF form using MIP solvers. PH algorithm is an efficient decomposition to heuristically solve the two-stage SMIP model. The solution process of the PH algorithm is stated in detail as follows. A penalty factor  $\rho > 0$  and a termination threshold  $\varepsilon$  are taken

as the input parameters.

PH algorithm for two-stage SMIP

*Step 1:* initialization. Let iteration counter  $k \leftarrow 0$  and multiplier  $(\mathbf{w}(s))^k \leftarrow \mathbf{0}$ . For each  $s = 1, 2, \dots, S$ , calculate  $((\mathbf{x}(s))^{k+1}, (\mathbf{y}(s))^{k+1}) := \arg \min_{\mathbf{x}(s), \mathbf{y}(s)} \{ \mathbf{c}^T \mathbf{x}(s) + (\mathbf{p}(s))^T \mathbf{y}(s) : (\mathbf{x}(s), \mathbf{y}(s)) \in \mathcal{Q}(s) \}$ .

*Step 2:* iteration update,  $k \leftarrow k + 1$ .

*Step 3:* aggregation. Calculate the weighted average of all subproblem solutions as  $\bar{\mathbf{x}}^k = \sum_s \pi^s (\mathbf{x}(s))^k$ .

*Step 4:* multiplier update, i.e.,  $(\mathbf{w}(s))^k = (\mathbf{w}(s))^{k-1} + \rho(\mathbf{x}(s)^k - \bar{\mathbf{x}}^k)$ ,  $s = 1, 2, \dots, S$ .

*Step 5:* decomposition. For each  $s = 1, 2, \dots, S$ , calculate  $((\mathbf{x}(s))^{k+1}, (\mathbf{y}(s))^{k+1}) := \arg \min_{\mathbf{x}(s), \mathbf{y}(s)} \{ \mathbf{c}^T \mathbf{x}(s) + (\mathbf{p}(s))^T \mathbf{y}(s) + (\mathbf{w}(s))^k \mathbf{x}(s) + \rho \| \mathbf{x}(s) - \bar{\mathbf{x}}^k \|_2^2 / 2 : (\mathbf{x}(s), \mathbf{y}(s)) \in \mathcal{Q}(s) \}$ .

*Step 6:* termination. Compute weighted distance  $\lambda^k = \sum_s \pi^s \| (\mathbf{x}(s))^{k+1} - \bar{\mathbf{x}}^k \|_2^2$ .

If  $\lambda^k \leq \varepsilon$ , the iteration stops; otherwise, return to *Step 2*.

Accordingly, each subproblem has significantly fewer binary decision variables than the original problem. Besides, all subproblems can be solved in parallel. Hence, the computational performance is improved. The number of variables and constraints for the original problem and each subproblem are compared in Table I.

TABLE I  
COMPLEXITY OF ORIGINAL PROBLEM AND EACH SUBPROBLEM

Item	Original problem	Subproblem
Binary variable	$x_{l,t}, x_{l,fr,t}^s, x_{l,to,t}^s, y_{b,t}^s, y_{g,t}^s, y_{w,t}^s, y_{d,t}^s$	$x_{l,t}, x_{l,fr,t}, x_{l,to,t}, y_{b,t}, y_{g,t}, y_{w,t}, y_{d,t}$
Number of binary variables	$(2L + B + G + W + D)ST + TL$	$(2L + B + G + W + D)T + TL$
Continuous variable	$P_{g,t}^s, P_{g,t,i}^s, P_{d,t,i}^s, P_{w,t,i}^s, \tilde{P}_{d,t,i}^s, \tilde{P}_{w,t,i}^s, \tilde{P}_{w,t,i}^s, P_{l,t,i}^s, P_{l,e,t,i}^s, \theta_{b,t,i}^s, \theta_{l,e,t,i}^s, \theta_{l,e,t,i}^s$	$P_{g,t}, P_{g,t,i}, P_{d,t,i}, P_{w,t,i}, \tilde{P}_{d,t,i}, \tilde{P}_{w,t,i}, \tilde{P}_{w,t,i}, P_{l,t,i}, P_{l,e,t,i}, \theta_{b,t,i}, \theta_{l,e,t,i}, \theta_{l,e,t,i}$
Number of continuous variables	$(11L + 2B + 3G + 5W + 5D)ST$	$(11L + 2B + 3G + 5W + 5D)T$
Number of constraints	$L + L(T - X_l)(X_l - 1) + T + 2LT + (16L + 4B + 4G + 6W + 6D + 1)ST$	$L + L(T - X_l)(X_l - 1) + T + 2LT + (16L + 4B + 4G + 6W + 6D + 1)T$

Note that the advantage of the PH algorithm increases as the number of scenarios increases.

The convergence of the PH algorithm can be accelerated by setting the proper penalty factor  $\rho$ . In [26], a method for selecting  $\rho$  is discussed:

$$\rho = \frac{c}{x_{\max,1} - x_{\min,1} + 1} \quad (48)$$

where  $x_{\max,1}$  and  $x_{\min,1}$  represent the maximum and minimum values of the obtained decisions in the *Step 1* of PH algorithm. Equation (48) exploits the fact that the PH algorithm performs best when the penalty factor is proportional to element unit cost  $c$ .

#### IV. CASE STUDY

In this section, case studies are presented to demonstrate the effectiveness of the proposed model. Simulations are modeled with YALMIP [31] and solved with Gurobi [32] in MATLAB. All experiments are implemented on a workstation, whose individual blade consists of two 3.0 GHz 24-Core Intel Xeon Gold 6248R processors and 256 GB of RAM.

##### A. Test System and Data

The modified IEEE RTS-79 system [33] is used as the test system. The load data of the 9<sup>th</sup> week are selected. The system and data are modified as follows.

1) The 400 MW nuclear power plants at bus 18 and bus 21 are replaced by 400 MW wind farms. The data of the other generation units remain unchanged. The rated power of each wind turbine generator is 5 MW. The cut-in, rated, and cut-out wind speeds of wind turbine generators are 3 m/s, 11 m/s, and 25 m/s, respectively. The relationship between wind speed and output power can be found in [34].

2) The rated capacities of lines 25, 26, and 27 are modified to 0.35 p.u.. The capacities of the remaining lines or branches are modified to 0.6 p.u..

Overall, the modified system consists of 2 wind farms, 30 conventional units, 20 load buses, 24 buses, and 38 transmission lines. The marginal costs of conventional units can be found in [35] and are reported in Table II. The costs of wind curtailment and load shedding are set as 100 \$/MW and 500 \$/MW [36], respectively.

TABLE II  
MARGINAL COSTS OF CONVENTIONAL UNITS

Unit type	Capacity (MW)	Marginal cost (\$/MW)
U12	12	56
U20	20	130
U50	50	0
U76	76	16
U100	100	43
U155	155	12
U197	197	48
U350	350	11

A total of three transmission lines need to be switched for maintenance. The maintenance data are given in Table III.

TABLE III  
MAINTENANCE DATA OF TRANSMISSION LINES

Line No.	Starting bus	End bus	Maintenance duration (hour)
18	Bus 11	Bus 13	24
25	Bus 15	Bus 21	24
30	Bus 17	Bus 18	24

##### B. Calculation Result

To investigate the effect of employing NTO during TMS, the following cases are studied.

Case 1: neither TMS nor NTO is considered. This case is set as the base case.

Case 2: only TMS is considered.

Case 3: both TMS and NTO are considered.

In Case 3, assume NTO can only be employed during the transmission maintenance period. Therefore, the cost of considering TMS and the benefits of introducing NTO can be observed more intuitively.

The scheduled maintenance periods in Case 2 and Case 3 are listed in Table IV. There is no load shedding in all cases. Therefore, the total cost consists of conventional generation cost and wind curtailment cost. The specific results can be found in Fig. 3.

TABLE IV  
SCHEDULED MAINTENANCE PERIODS IN CASE 2 AND CASE 3

Line No.	Scheduled maintenance period (hour)	
	Case 2	Case 3
18	23-46	66-89
25	140-163	90-113
30	82-105	145-168

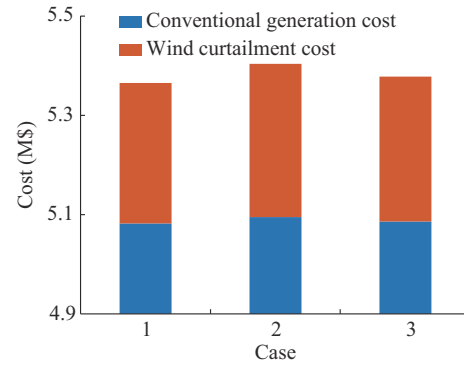


Fig. 3. Specific results of three cases.

Figure 3 shows that Case 1 has the least wind curtailment cost and total cost, while Case 2 has the largest wind curtailment cost and total cost. In addition, the total cost of Case 3 is lower than that of Case 2. The cost reduction can be attributed to the adoption of NTO, which decreases the wind curtailment and enables higher outputs of low-cost units.

Furthermore, it can be found that the transmission network topology remains consistent except for the maintenance period. Figure 4 shows that the discrepancy between wind curtailments of Case 1 and Case 2 can be regarded as the cost considering maintenance, and the discrepancy between wind curtailments of Case 2 and Case 3 can be regarded as the benefits from introducing NTO. It can be concluded that NTO reduces the negative impact of transmission maintenance on wind accommodation by 65.49% during the maintenance.

##### C. Impacts of TMS and NTO on Wind Curtailment

To intuitively observe the impacts of TMS and NTO on wind curtailment, the difference of wind curtailment of Case 2 and Case 3 compared with that of Case 1 is drawn in the form of stairs, as shown in Fig. 5.

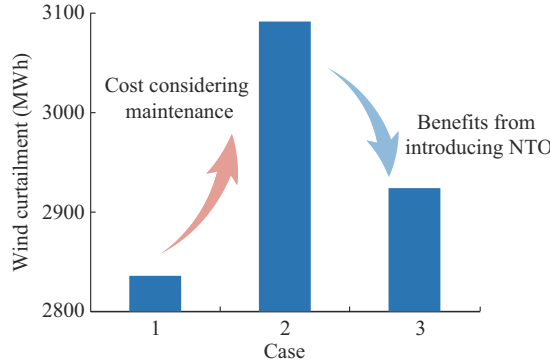


Fig. 4. Illustration of impacts of maintenance and NTO on wind curtailment.

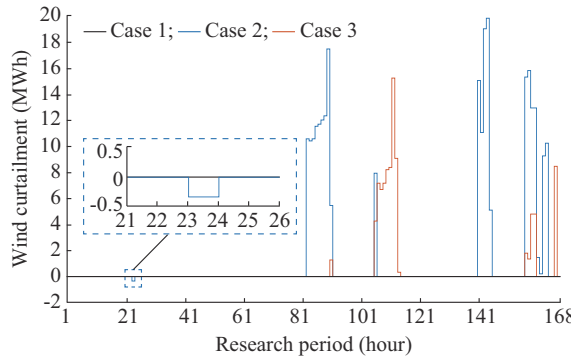


Fig. 5. Difference of wind curtailment of Case 2 and Case 3 compared with that of Case 1 in each period.

First, it can be found that the wind curtailment of Case 2 is slightly less than that of Case 1 during the maintenance period of line 18. The reason is that the line needs to be disconnected during the maintenance, which can be regarded as the outage of the line. On the other hand, the transmission network topology in Case 2 is better than that in Case 1 in the 23<sup>th</sup> hour. Although the maintenance will change the network topology, the proper arrangement of maintenance periods will minimize its impact on system economic operation.

Then, it can be observed that the discrepancy between wind curtailments of Case 1 and Case 2 or Case 3 mainly occurs during the maintenance periods of line 25 and line 30. Both lines are directly connected to wind farms and their maintenance will have a large impact on the wind curtailment.

Finally, the maintenance of line 25 and line 30 leads to a substantial increase in wind curtailment. However, the wind curtailment can be alleviated through NTO. As mentioned above, these two lines are directly connected to the wind farms. Therefore, the maintenance of these two lines will result in fewer power transmission channels of wind farms and a large amount of wind power cannot be used to supply the system load, resulting in a sharp increase in wind curtailment. When the network topology is optimized, the distribution of the power flow can be adjusted and the utilization rates of the transmission lines directly connected to the wind farms can be adjusted, thereby improving the accommodation rate of wind power.

#### D. Analysis of Effect of NTO on Alleviating Transmission Congestion

To explore the effect of NTO on alleviating the transmission congestion, the utilization rate of transmission lines when line 30 is under maintenance is compared using the form of heat map in Fig. 6. It can be observed that the distribution of line flow is adjusted through NTO.

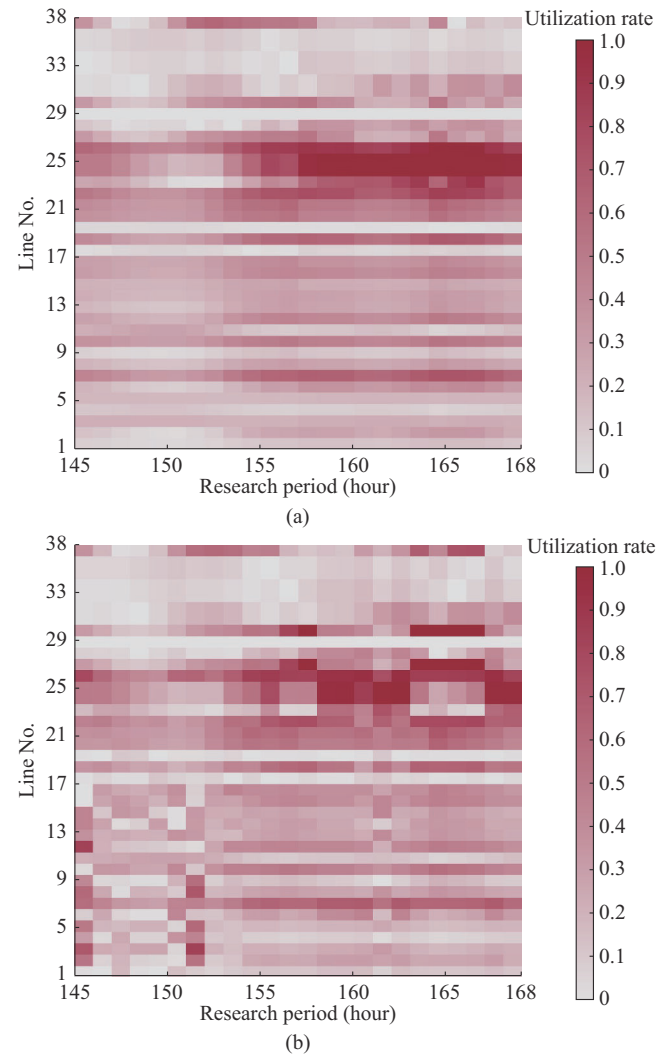


Fig. 6. Utilization rate of transmission lines when line 30 is under maintenance. (a) Situation without NTO. (b) Situation with NTO.

Line 25, line 26, and line 38 are important lines for delivering wind power. However, it can be observed from Fig. 6(a) that both line 25 and line 26 are blocked during 158-167 hours. This will inevitably lead to a significant increase in wind curtailment.

In Fig. 6(b), the utilization rate of line 25 and line 26 drops slightly and the utilization rate of line 38 increases significantly. This result indicates that the NTO has a positive impact on relieving transmission congestion and can improve the wind power accommodation.

#### E. Analysis of Computational Performance

The computation time of the brute-force (BF) approach, i.e., solving the EF of the proposed model directly using the

Gurobi solver, and the PH algorithm is compared with different numbers of scenarios, as shown in Table V.

TABLE V  
COMPUTATION TIME OF BF APPROACH AND PH ALGORITHM

Number of scenarios	Computation time (s)	
	BF	PH
2	864.7	521.1
4	1958.0	731.7
6	9524.0	1346.8
8	48931.9	1726.4
10	> 200000.0	6727.0

Though both BF approach and PH algorithm can solve the problem, their computation time is different. In the case of two scenarios, the computation time of the BF approach is close to that of the PH algorithm. However, as the number of scenarios increases, the computation time of BF approach increases faster than that of the PH algorithm. The BF approach cannot find a satisfactory solution in 200000 s in the case of 10 scenarios. It fully reflects the advantage of the PH algorithm when more scenarios are included in the formulation.

#### F. Analysis of Split Bus-bars During Maintenance

In the test system, there are a total of nine bus-bars that can be split. However, only four bus-bars need to be split during the maintenance period. They are bus-bar 9, bus-bar 10, bus-bar 16, and bus-bar 21, respectively. In addition, 5 periods do not require the split of bus-bars during the maintenance period. It proves that NTO is not always necessary to the economic operation of the system. During the maintenance period of various transmission lines, the split times of each bus-bar are divided by the total split time to derive the proportion results, which are shown in Fig. 7.

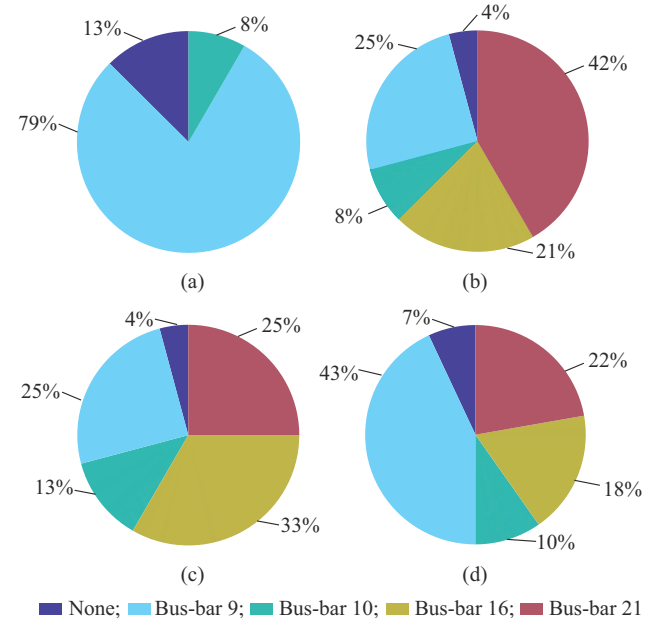


Fig. 7. Proportion of split times of each bus-bar during maintenance period of various transmission lines. (a) Line 18. (b) Line 25. (c) Line 30. (d) Total.

It can be observed that the components of bus-bar split times are significantly different in the maintenance period of various transmission lines. Therefore, the optimal transmission network topology is not always the same, which is determined by the profile of power generation and load demand. Taking bus-bar 9 as an example, the 9 situations after splitting are shown in Fig. 8. The situations 1 and 2 occur the most. Although it is difficult to capture the optimal transmission network topology, a suboptimal one can be obtained within a limited time according to the results in Fig. 7 and Fig. 8.

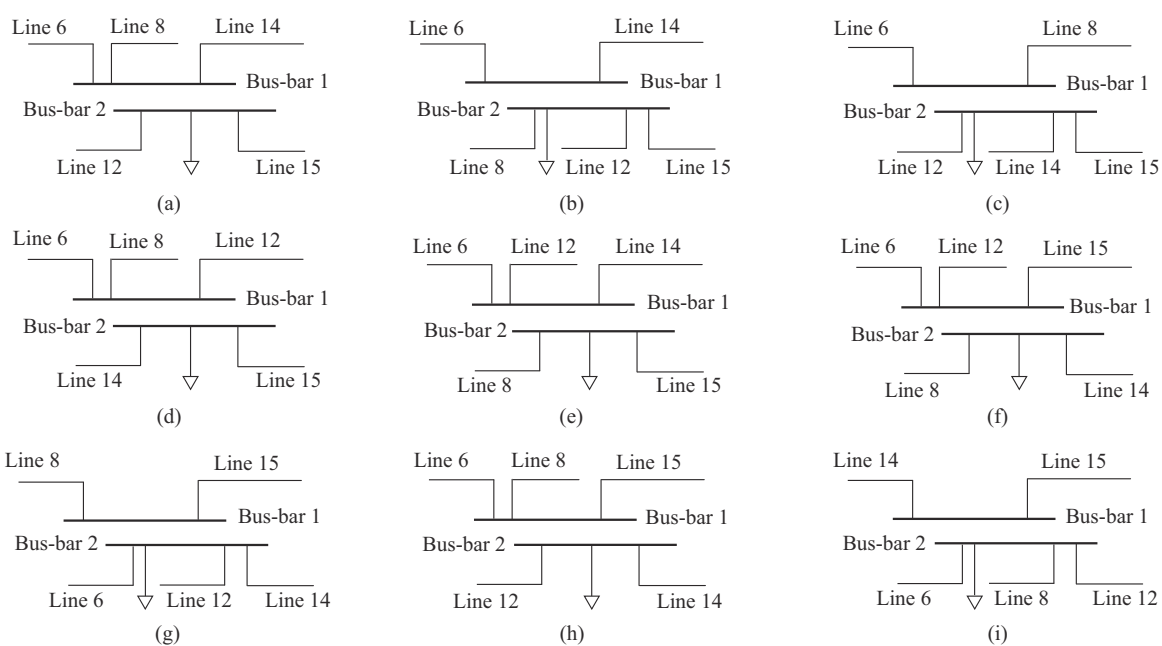


Fig. 8. Situations after splitting of bus-bar 9. (a) Situation 1. (b) Situation 2. (c) Situation 3. (d) Situation 4. (e) Situation 5. (f) Situation 6. (g) Situation 7. (h) Situation 8. (i) Situation 9.

## V. CONCLUSION

This paper proposes an innovative short-term TMS approach. A two-stage SMIP model is established to co-optimize the TMS and NTO. The first stage is to make TMS decisions and the second stage is to determine the optimal transmission network topology during the maintenance period. The modified IEEE RTS-79 system is applied for case studies. The conclusions obtained from the case studies are as follows.

1) The network topology will be changed by the transmission maintenance. Therefore, the negative impact of maintenance on the system economic operation can be minimized if it is properly scheduled.

2) The maintenance of transmission lines that are directly connected to wind farms will lead to a large amount of wind curtailment.

3) The optimization of network topology during the maintenance period can significantly relieve the transmission congestion and consequently reduce the wind curtailment.

## REFERENCES

- [1] Y. Gu, L. Xie, B. Rollow *et al.*, “Congestion-induced wind curtailment: sensitivity analysis and case studies,” in *Proceedings of 2011 North American Power Symposium*, Boston, USA, Aug. 2011, pp. 1-7.
- [2] Y. Gu and L. Xie, “Fast sensitivity analysis approach to assessing congestion induced wind curtailment,” *IEEE Transactions on Power Systems*, vol. 29, no. 1, pp. 101-110, Sept. 2013.
- [3] S. Chellam and S. Kalyani, “Power flow tracing based transmission congestion pricing in deregulated power markets,” *International Journal of Electrical Power & Energy Systems*, vol. 83, pp. 570-584, Dec. 2016.
- [4] A. Froger, M. Gendreau, J. E. Mendoza *et al.*, “Maintenance scheduling in the electricity industry: a literature review,” *European Journal of Operational Research*, vol. 251, no. 3, pp. 695-706, Jun. 2016.
- [5] M. K. C. Marwali and S. M. Shahidehpour, “A deterministic approach to generation and transmission maintenance scheduling with network constraints,” *Electric Power Systems Research*, vol. 47, no. 2, pp. 101-113, Oct. 1998.
- [6] M. K. C. Marwali and S. M. Shahidehpour, “Long-term transmission and generation maintenance scheduling with network, fuel and emission constraints,” *IEEE Transactions on Power Systems*, vol. 14, no. 3, pp. 1160-1165, Aug. 1999.
- [7] T. Geetha and K. S. Swarup, “Coordinated preventive maintenance scheduling of GENCO and TRANSCO in restructured power systems,” *International Journal of Electrical Power & Energy Systems*, vol. 31, no. 10, pp. 626-638, Nov. 2009.
- [8] Y. Wang, H. Zhong, Q. Xia *et al.*, “An approach for integrated generation and transmission maintenance scheduling considering  $N-1$  contingencies,” *IEEE Transactions on Power Systems*, vol. 31, no. 3, pp. 2225-2233, May 2016.
- [9] Y. Fu, M. Shahidehpour, and Z. Li, “Security-constrained optimal coordination of generation and transmission maintenance outage scheduling,” *IEEE Transactions on Power Systems*, vol. 22, no. 3, pp. 1302-1313, Aug. 2007.
- [10] Y. Fu, Z. Li, M. Shahidehpour *et al.*, “Coordination of midterm outage scheduling with short-term security-constrained unit commitment,” *IEEE Transactions on Power Systems*, vol. 24, no. 4, pp. 1818-1830, Nov. 2009.
- [11] M. Abirami, S. Ganeshan, S. Subramanian *et al.*, “Source and transmission line maintenance outage scheduling in a power system using teaching learning based optimization algorithm,” *Applied Soft Computing*, vol. 21, pp. 72-83, Aug. 2014.
- [12] Y. Wang, Z. Li, M. Shahidehpour *et al.*, “Stochastic co-optimization of midterm and short-term maintenance outage scheduling considering covariates in power systems,” *IEEE Transactions on Power Systems*, vol. 31, no. 6, pp. 4795-4805, Nov. 2016.
- [13] K. Warwick, A. Ekwue, R. Aggarwal *et al.*, *Artificial Intelligence Techniques in Power Systems*. London, UK: The Institution of Engineering and Technology, 1997.
- [14] M. K. C. Marwali and S. M. Shahidehpour, “Short-term transmission line maintenance scheduling in a deregulated system,” in *Proceedings of the 21st International Conference on Power Industry Computer Applications*, Santa Clara, USA, May 1999, pp. 31-37.
- [15] H. Pandzic, A. J. Conejo, I. Kuzle *et al.*, “Yearly maintenance scheduling of transmission lines within a market environment,” *IEEE Transactions on Power Systems*, vol. 27, no. 1, pp. 407-415, Feb. 2012.
- [16] J. Liu, M. Kazemi, A. Motamed *et al.*, “Security-constrained optimal scheduling of transmission outages with load curtailment,” *IEEE Transactions on Power Systems*, vol. 33, no. 1, pp. 921-931, Jan. 2018.
- [17] B. Li, X. Han, and S. Wang, “Robust optimal coordination of transmission maintenance scheduling with unit commitment considering the interval uncertainty of nodal demands and wind power,” *Proceeding of the CSEE*, vol. 38, no. 20, pp. 6001-6011, Oct. 2018.
- [18] Z. Yang, H. Zhong, Q. Xia *et al.*, “Review and prospect of transmission topology optimization,” *Proceedings of the CSEE*, vol. 36, no. 2, pp. 426-434, Jan. 2016.
- [19] E. B. Fisher, R. P. O'Neill, and M. C. Ferris, “Optimal transmission switching,” *IEEE Transactions on Power Systems*, vol. 23, no. 3, pp. 1346-1355, Aug. 2008.
- [20] W. Shao and V. Vittal, “Corrective switching algorithm for relieving overloads and voltage violations,” *IEEE Transactions on Power Systems*, vol. 20, no. 4, pp. 1877-1885, Oct. 2005.
- [21] A. A. Mazi, B. F. Wollenberg, and M. H. Hesse, “Corrective control of power system flows by line and bus-bar switching,” *IEEE Transactions on Power Systems*, vol. 1, no. 3, pp. 258-264, Aug. 1986.
- [22] G. Granelli, M. Montagna, F. Zanellini *et al.*, “Optimal network reconfiguration for congestion management by deterministic and genetic algorithms,” *Electric Power Systems Research*, vol. 76, no. 6-7, pp. 549-556, Nov. 2005.
- [23] J. Wu and K. W. Cheung, “Incorporating optimal transmission switching in day-ahead unit commitment and scheduling,” in *Proceedings of 2015 IEEE PES General Meeting*, Denver, USA, Jul. 2015, pp. 1-5.
- [24] M. Heidarifar and H. Ghasemi, “A network topology optimization model based on substation and node-breaker modeling,” *IEEE Transactions on Power Systems*, vol. 31, no. 1, pp. 247-255, Jan. 2016.
- [25] R. T. Rockafellar and R. J.-B. Wets, “Scenarios and policy aggregation in optimization under uncertainty,” *Mathematics of Operations Research*, vol. 16, no. 1, pp. 119-147, Feb. 1991.
- [26] J.-P. Watson and D. L. Woodruff, “Progressive hedging innovations for a class of stochastic mixed-integer resource allocation problems,” *Computational Management Science*, vol. 8, no. 4, pp. 355-370, Nov. 2011.
- [27] S. Ma, L. Su, Z. Wang *et al.*, “Resilience enhancement of distribution grids against extreme weather events,” *IEEE Transactions on Power Systems*, vol. 33, no. 5, pp. 4842-4853, Sept. 2018.
- [28] J. Kim and Y. Dvorkin, “Enhancing distribution system resilience with mobile energy storage and microgrids,” *IEEE Transactions on Smart Grid*, vol. 10, no. 5, pp. 4996-5006, Sept. 2019.
- [29] National Research Council. *Terrorism and the Electric Power Delivery System*. Washington DC, USA: National Academies Press, 2012.
- [30] L. Wu, M. Shahidehpour, and T. Li, “Stochastic security-constrained unit commitment,” *IEEE Transactions on Power Systems*, vol. 22, no. 2, pp. 800-811, May 2007.
- [31] J. Lofberg, “YALMIP: a toolbox for modeling and optimization in MATLAB,” in *Proceedings of 2004 IEEE International Conference on Robotics and Automation*, Taipei, China, Sept. 2004, pp. 284-289.
- [32] Gurobi Optimization. (2021, Jan.). Gurobi optimizer. [Online]. Available: <http://www.gurobi.com>
- [33] P. Subcommittee, “IEEE reliability test system,” *IEEE Transactions on Power Apparatus and Systems*, vol. PAS-98, no. 6, pp. 2047-2054, Nov. 1979.
- [34] P. Giorsetto and K. F. Utsurogi, “Development of a new procedure for reliability modeling of wind turbine generators,” *IEEE Transactions on Power Apparatus and Systems*, vol. PAS-102, no. 1, pp. 134-143, Jan. 1983.
- [35] H. Nemati, M. A. Latify, and G. R. Yousefi, “Coordinated generation and transmission expansion planning for a power system under physical deliberate attacks,” *International Journal of Electrical Power & Energy Systems*, vol. 96, pp. 208-221, Mar. 2018.
- [36] E. Du, N. Zhang, C. Kang *et al.*, “Scenario map based stochastic unit commitment,” *IEEE Transactions on Power Systems*, vol. 33, no. 5, pp. 4694-4705, Sept. 2018.

Weixin Zhang received the B. S. degree from Chongqing University, Chongqing, China, in 2018. He is currently pursuing the Ph.D. degree in

Chongqing University. His research interests include power system risk assessment and optimization.

**Bo Hu** received the Ph.D. degree in electrical engineering from Chongqing University, Chongqing, China, in 2010, where he is currently a Professor with the School of Electrical Engineering. He is an Editor of the IEEE Transactions on Power Systems. His research interests include power system reliability and parallel computing techniques in power systems.

**Kaigui Xie** received the Ph.D. degree in power system and its automation from Chongqing University, Chongqing, China, in 2001, where he is currently a Full Professor with the School of Electrical Engineering. He is an Associate Editor of IET Proceedings: Generation, Transmission and Distribution. His research interests include power system reliability, planning, and analysis.

**Changzheng Shao** received the B.S. degree in electrical engineering from Shandong University, Jinan, China and the Ph.D. degree in electrical engineering from Zhejiang University, Hangzhou, China, in 2015 and 2020, respectively. He is currently an Assistant Professor at Chongqing University, Chongqing, China. His research interests include the operation optimization and reliability evaluation of integrated energy system.

**Tao Niu** received the B.S. and Ph.D. degrees from the Department of Electrical Engineering, Tsinghua University, Beijing, China, in 2014 and 2019,

respectively. He is currently an Assistant Professor with Chongqing University, Chongqing, China. His research interests include voltage security region, automatic reactive power voltage control, renewable generation integration, and reactive power analysis of hybrid AC/DC system.

**Jiahao Yan** received the B.S. degree from Hefei University of Technology, Hefei, China, in 2016. He is currently pursuing the Ph.D. degree in Chongqing University, Chongqing, China. His research interests include power system risk assessment and optimization.

**Lvbin Peng** received B.S. degree in Hefei University of Technology, Hefei, China, in 2014. He is currently a Ph.D. candidate in the School of Electrical Engineering, Chongqing University, Chongqing, China. His research interests include power system reliability and planning.

**Maosen Cao** received the B. S. degree in electrical engineering from the Southwest Jiaotong University, Chengdu, China, in 2018. He is currently pursuing the Ph.D. degree with Chongqing University, Chongqing, China. His research interests include reliability assessment and optimization of the integrated energy system.

**Yue Sun** received the B.S. degree from Guizhou University, Guizhou, China, in 2019. He is currently working toward the M.S. degree with Chongqing University, Chongqing, China. His research interests include power system operation optimization and reliability.